In vivo imaging of cortical pathology in multiple sclerosis using ultra-high field MRI

🐇 📖

C. Mainero, MD, PhD
T. Benner, PhD
A. Radding
A. van der Kouwe, PhD
R. Jensen, MD
B.R. Rosen, MD, PhD*
R.P. Kinkel, MD*

Address correspondence and reprint requests to Dr. Caterina Mainero, Athinoula Martinos Center for Biomedical Imaging, Massachusetts General Hospital, 149 13th St., Charlestown, MA 02129
caterina@nmr.mgh.harvard.edu

ABSTRACT

Objective: We used ultra-high field MRI to visualize cortical lesion types described by neuropathology in 16 patients with multiple sclerosis (MS) compared with 8 age-matched controls; to characterize the contrast properties of cortical lesions including T2*, T2, T1, and phase images; and to investigate the relationship between cortical lesion types and clinical data.

Methods: We collected, on a 7-T scanner, 2-dimensional fast low-angle shot (FLASH)-T2*-weighted spoiled gradient-echo, T2-weighted turbo spin-echo (TSE) images ($0.33 \times 033 \times 1$ mm^3), and a 3-dimensional magnetization-prepared rapid gradient echo.

Results: Overall, 199 cortical lesions were detected in patients on both FLASH-T2* and T2-TSE scans. Seven-tesla MRI allowed for characterization of cortical plaques into type I (leukocortical), type II (intracortical), and type III/IV (subpial extending partly or completely through the cortical width) lesions as described histopathologically. Types III and IV were the most frequent type of cortical plaques (50.2%), followed by type I (36.2%) and type II (13.6%) lesions. Each lesion type was more frequent in secondary progressive than in relapsing–remitting MS. This difference, however, was significant only for type III/IV lesions. T2*-weighted images showed the highest, while phase images showed the lowest, contrast-to-noise ratio for all cortical lesion types. In patients, the number of type III/IV lesions was associated with greater disability ($p < 0.02$ by Spearman test) and older age ($p < 0.04$ by Spearman test).

Conclusions: Seven-tesla MRI detected different histologic cortical lesion types in our small multiple sclerosis (MS) sample, suggesting, if validated in a larger population, that it may prove a valuable tool to assess the contribution of cortical MS pathology to clinical disability. *Neurology*® 2009;73:941–948

GLOSSARY

ANOVA = analysis of variance; **BN** = background noise; **CNR** = contrast-to-noise ratio; **DIR** = double-inversion recovery; **EDSS** = Expanded Disability Status Scale; **FLAIR** = fluid-attenuated inversion recovery; **FLASH** = fast low-angle shot; **GM** = gray matter; **MPRAGE** = magnetization-prepared rapid gradient echo; **MR** = magnetic resonance; **MS** = multiple sclerosis; **NACGM** = normal-appearing cortical gray matter; **RF** = radiofrequency; **ROI** = region of interest; **RRMS** = relapsing-remitting multiple sclerosis; **SNR** = signal-to-noise ratio; **SPMS** = secondary progressive multiple sclerosis; **TA** = time of acquisition; **TE** = echo time; **TR** = repetition time; **TSE** = turbo spin-echo; **WM** = white matter.

Although cortical lesions were identified as a common finding in multiple sclerosis (MS) from the earliest pathologic studies,[1-3] their significance was underestimated until recent histopathologic data revealed that they constitute a substantial proportion of the total brain MS lesion load.[4,5]

The ability of standard field strength scanners (1.5 T, 3 T) to detect and characterize cortical MS pathology is still significantly lower than neuropathology.[6] Ultra-high field systems (7 T to 9.4 T) allow a 2- to 3-fold improvement in image signal-to-noise ratio (SNR) over 3-T MRI.[7] Advances in multichannel radiofrequency (RF) technology provide an additional 2- to 6-fold improvement in SNR, with the greatest gains in the cortex.[8]

Supplemental data at www.neurology.org

Editorial, page 918

Data at ultra-high field strengths also demonstrate greatly enhanced T2* contrast, potentially providing a novel tool for lesion detection.[9] Additionally, previous findings in MS using phase reconstruction at 7-T techniques revealed in some white matter (WM) lesions a characteristic high-susceptibility (χ) ring not readily visible on magnitude T2* images.[10] The high-susceptibility ring is thought to reflect iron-rich macrophages[11] and the extent of tissue inflammation.

We assessed the ability of 7-T MRI combined with multichannel RF technology to 1) visualize in vivo all cortical MS lesion types described histopathologically; 2) characterize the contrast properties at this field strength of cortical lesions on T2*-, T2-, T1-weighted, and phase images to assess which magnetic resonance (MR) contrasts are more sensitive to cortical pathology; and 3) investigate the relationship between cortical lesion types, clinical data, and WM lesion load.

METHODS **Subjects.** We enrolled 16 consecutive patients (9 women; mean ± SD age of 38.8 ± 12.4 years; mean ± SD disease duration of 10.2 ± 7.4 years) with a diagnosis of MS according to the McDonald criteria.[12] Nine patients had relapsing–remitting MS (RRMS), and 7 patients secondary progressive MS (SPMS). Disability was assessed using the Expanded Disability Status Scale (EDSS),[13] and the median (range) EDSS was 3.0 (1.0–6.5). Patients included in the study had to be relapse-free at least 3 months before study entry and without corticosteroid treatment for at least a month preceding study initiation. All patients except one had received disease-modifying agents for at least 3 months before the MRI. Eight age-matched healthy subjects (4 women, mean ± SD age of 33.4 ± 10 years) were included as controls. General exclusion criteria were significant medical, psychiatric, or neurologic history (other than MS for patients).

Standard protocol approvals, registrations, and patient consents. The local ethics committee of our institution approved all experimental procedures of the study, and written informed consent was obtained from each study participant.

Data acquisition. Subjects were scanned on a human 7-T scanner (Siemens, Erlangen, Germany) using an in-house developed 8-channel (5 patients and 2 controls) or 32-channel phased array coil (all remaining participants). We collected 2-dimensional fast low-angle shot (FLASH)-T2* spoiled gradient-echo weighted images (repetition time [TR]/echo time [TE] = 1,000/22 msec, flip angle = 55°, field of view = 168 × 192 voxels, bandwidth = 30 Hz/px, 20 × 1-mm-thick slices, in-plane resolution: 330 × 330 μm^2, time of acquisition [TA]: approximately 8 minutes), and T2-turbo spin-echo (TSE) (TR/TE = 6,890/78 msec, turbo factor = 9, 2 averages, TA: approximately 6 minutes) with the same resolution and orientation as FLASH-T2* scans. For each modality, 2 to 3 slabs were acquired, allowing coverage of the supratentorial brain. A 3-dimensional magnetization-prepared rapid gradient echo (MPRAGE) (TR/TE/inversion time = 2,600/3.26/1,100 msec, bandwidth = 205 Hz/px, 1.5-mm-thick slices, in-plane resolution: 600 × 600 μm^2, TA: approximately 5 minutes) oriented as FLASH-T2* and T2-TSE scans was also acquired. Shimming was performed before anatomic scanning to minimize magnetic field B_0 inhomogeneities.

Data processing. Seven-tesla data were processed to 1) visually inspect images for the presence and characterization of focal cortical lesions; 2) assess cortical lesions contrast-to-noise ratio (CNR) at different MR contrasts, including T2*, T2, T1, and phase; and 3) quantify the load of WM hyperintensities on FLASH-T2* scans.

Anatomic scans were corrected for coil sensitivity profiles using a nonuniformity correction algorithm.[14] Phase images were postprocessed using PRELUDE (http://www.fmrib.ox.ac.uk/fsl)[15] to generate a full-range phase image. PRELUDE is an automatic phase unwrapping algorithm that segments the image into regions of low phase variation and merges regions by adding 2π offsets to minimize phase differences over the boundary. Regions outside the brain were excluded from the unwrapping algorithm using the magnitude mask image. An edge-filled, low-pass filtered (2-mm gaussian filter) phase image was then subtracted from the unwrapped global phase image to remove the large background field and highlight local anatomy. This method preserves the high-resolution anatomy of the native data sets while eliminating low spatial frequency phase distortions due to B_0/B_1 inhomogeneities.

Cortical lesions were defined as focal cortical hyperintensities on FLASH-T2* magnitude and T2-TSE scans by 2 independent experienced observers blinded to demographic and clinical characteristics of subjects but obviously aware of WM lesions of patients. The following types of cortical plaques were identified according to previous neuropathologic descriptions[5,16,17]: 1) type I (leukocortical) lesions that extend across both WM and gray matter (GM); 2) type II (intracortical) lesions located within the cerebral cortex; 3) type III and type IV (subpial) lesions, extending from pial surface to cortical layers 3 and 4 or through the entire width of the cortex but without involving subcortical WM. The interrater variability in the number of all cortical lesions and of each histopathological type was calculated as the square root of the variance (SD) of the measurements divided by the corresponding mean, and resulted <0.1%. Cortical lesions were considered for further analyses only if there was full consensus between the 2 observers.

Table	Characterization of focal cortical lesion types at 7 T in 16 patients with multiple sclerosis: Comparison with neuropathology							
7-T MRI			**RRMS (n = 9)**		**SPMS (n = 7)**		**Pathology (study 1*), %**	**Pathology (study 2*), %**
	%	**(n)**	**Mean ± SE**	**Range**	**Mean ± SE**	**Range**		
All types	100	(199)	9.4 ± 2.2	2–21	19 ± 6.9	8–53	100	100
Type I	36.2	(72)	3.9 ± 1.6	1–16	6.2 ± 4.0	0–26	34	38
Type II	13.6	(27)	1.1 ± 0.4	0–3	2.8 ± 1.5	0–10	16	18
Type III/IV	50.2	(100)	4.4 ± 1.3	0–11	10 ± 2.3	4–17[†]	50	44

*Study 1 (5); study 2 (21).
[†] $p < 0.03$ by Mann–Whitney U test.
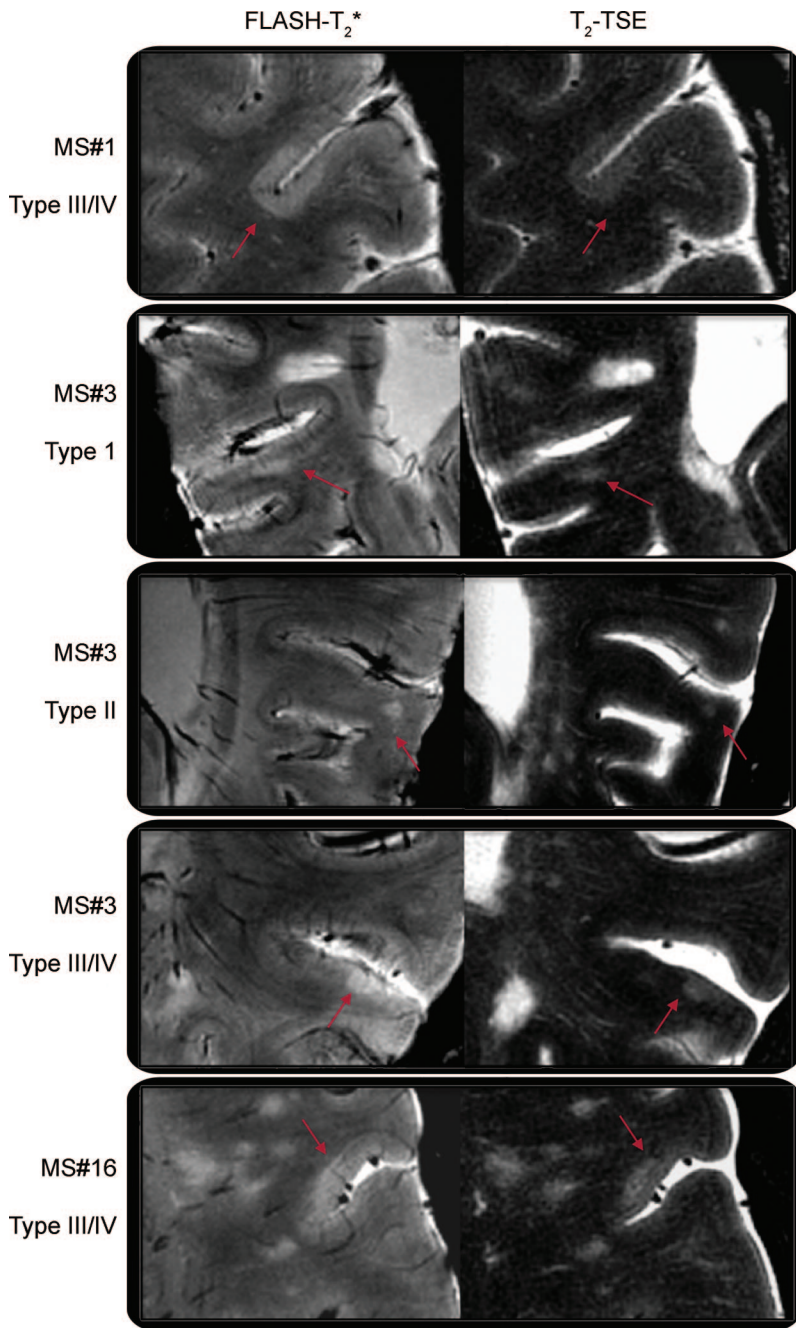RRMS = relapsing-remitting multiple sclerosis; SPMS = secondary progressive multiple sclerosis.

Illustration of different types of cortical lesions (type I: leukocortical; type II: intracortical; types III and IV: subpial lesions extending partly or all the way through the width of the cortex but not to subcortical white matter) on both fast low-angle shot (FLASH)-T2* and T2-turbo spin-echo (TSE) images in 1 patient with relapsing–remitting multiple sclerosis (MS#1, type IV lesion) and 2 patients with secondary progressive multiple sclerosis (MS#3 and MS#16) scanned at 7 T. Cortical plaques generally showed greater visible contrast on FLASH- T2* scans than on T2-TSE images.

The CNR of the different types of cortical lesions was calculated on data from 5 patients (3 with SPMS, 2 with RRMS). For each image (FLASH-T2*, T2-TSE, T1), regions of interest (ROIs; approximately 24 mm^3) were placed in 15 lesions (5 leukocortical, 5 intracortical, and 5 subpial), in adjacent ROIs of normal-appearing cortical GM (NACGM), and in ROIs outside the brain, away from imaging artifacts (background noise [BN]). The CNR of the different types of cortical lesions was calculated

as the following: $(S_{LES} - S_{NACGM})/BN$, where S_{LES} and S_{CNAGM} represent the mean signal intensities in cortical lesions (S_{LES}) and in adjacent NACGM (S_{CNAGM}). For phase images, the CNR was calculated according to the formula described above using the same cortical lesions and NACGM ROIs used for all the other images, but where BN was calculated as the variance of signal intensity in NACGM ROIs because the actual variance in phase would be meaningless for background (zero signal) regions.
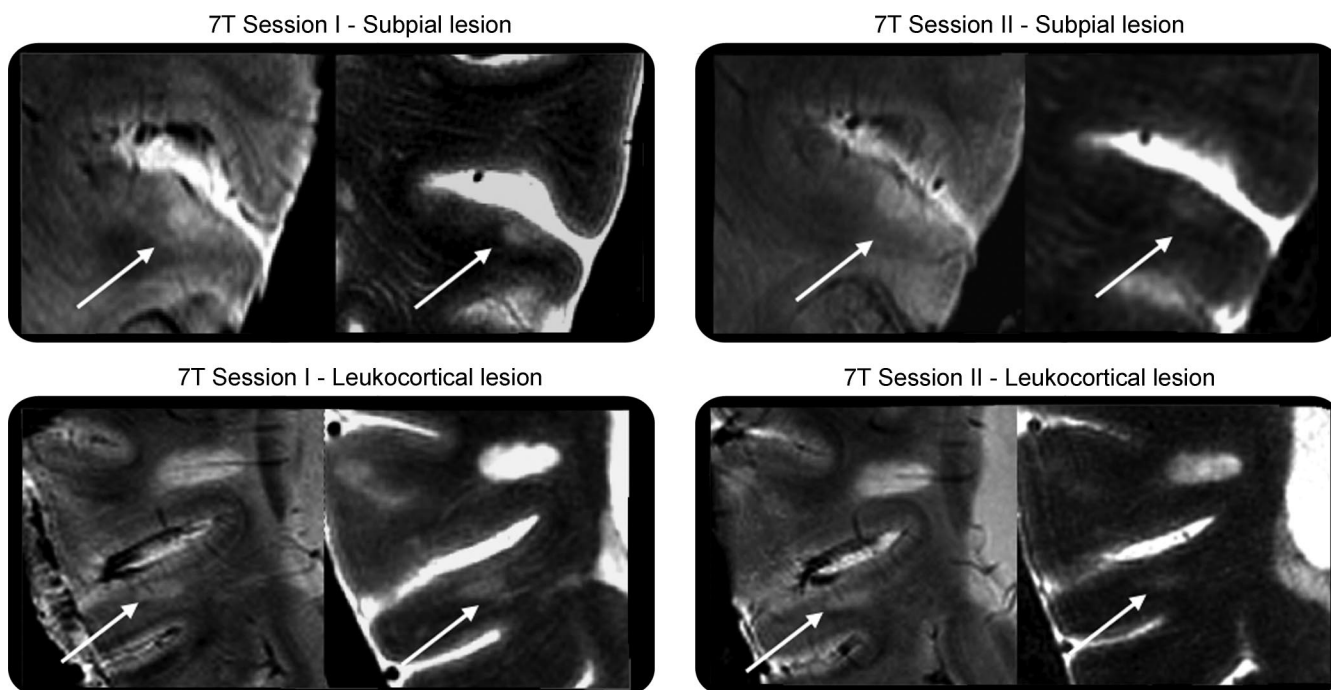
Finally, in each patient on FLASH-T2* scans, we calculated as previously described[18] the lesion load of WM hyperintensities using the software Alice (Hayden Image Processing Solutions) based on a local threshold contouring technique.

Statistics. Statistical analysis was performed using SPSS version 16 (SPSS Inc., Chicago, IL). Differences in the number of cortical lesions, including the different histopathologic types, between patients with RRMS and SPMS and between sexes were evaluated by Mann–Whitney U test. Differences in CNR of cortical lesions between the different MR contrasts were assessed using analysis of variance (ANOVA) with post hoc Bonferroni correction. The relationship between the total number of cortical plaques and of each cortical lesion type, WM lesion load, and demographic and clinical characteristics of patients was assessed using the Spearman ρ correlation coefficient.

RESULTS Lesion types and distribution. Imaging at 7 T was well tolerated in all subjects: no subjects reported any sustained discomfort or disorientation within the 7-T scanner, beyond the occasional short-lived description of a mild "turning" sensation as subjects were entering or exiting the scanner. In controls, we did not find cortical abnormalities on any scan. Cortical plaques were identified in all patients included in the study, with each patient showing at least 2 lesions. Overall, we detected 199 cortical lesions on both FLASH-T2* and T2-TSE scans, and the mean $\pm$ SE (range) number of cortical lesions was 13.3 $\pm$ 3.1 (2–53). Although women showed more cortical lesions than men (mean $\pm$ SE: 16.4 $\pm$ 5.8 vs 9.7 $\pm$ 1.4), this difference was not significant.

Type III and IV subpial lesions were the most frequent type of cortical plaques observed (50.2%), followed by type I leukocortical lesions (36.2%) and type II intracortical lesions (13.6%). The ratio of lesion types seen on 7-T scans was nearly identical to that documented by histology (table). Cortical plaques, including type I, II, or III/IV, were more frequent in patients with SPMS compared with patients with RRMS (table). This difference was significant only for subpial lesions (table). Figure 1 shows examples of different cortical lesion types on FLASH, T2* magnitude, and T2-TSE scans.

Cortical lesions were predominantly located in the frontal cortex (n = 106), including prefrontal areas but also the motor cortex (figure e-1 on the *Neurology*® Web site at www.neurology.org), in the parietal (n = 47) and temporal cortex (n = 29) of both hemispheres. Few cortical lesions were observed

Figure 2 Reproducibility of 7-T MRI in disclosing cortical multiple sclerosis pathology

7T Session I - Subpial lesion

7T Session II - Subpial lesion

7T Session I - Leukocortical lesion

7T Session II - Leukocortical lesion

Example of reproducibility of 7-T MRI in detecting different cortical lesion types (subpial and leukocortical) in a patient with secondary progressive multiple sclerosis. In each rectangle, left image is fast low-angle shot-T2* and right image is turbo spin-echo.

in the occipital cortex (n = 17). In some patients, on FLASH-T2* magnitude images, in addition to focal subpial lesions, we observed band-like areas of hyperintensity that involved the outer cortical laminae and extended over an entire gyrus or multiple gyri, resulting in an extensive involvement of the cortex (figure e-2).

A patient with SPMS (woman, aged 48 years) and a control (man, aged 52 years) were scanned twice on the 7 T within a month interval, using the same procedures described above. In the first scan, FLASH-T2* and T2-TSE scans demonstrated the presence of 4 type I, 4 type II, and 5 type III/IV lesions in the patient with SPMS and no lesions in the control. Subsequent scanning disclosed the same lesions in the patient with SPMS on both scan protocols and still no lesions in the control. In the patient with SPMS, no new lesions were apparent across this time interval (figure 2).

Magnitude and phase in characterizing cortical lesions. Focal cortical hyperintensities identified on FLASH-T2* magnitude scans were visually inspected on phase images. Seven of the 16 patients (4 with RRMS and 3 with SPMS) showed phase hypointensities (susceptibility ring) in 15 of 72 (approximately 21%) leukocortical plaques. In 12 of these 15 leukocortical lesions, the hypointense ring was also evident directly on magnitude images, whereas in the remaining 3 lesions, it was present only on phase im-

ages. The subpial and intracortical pathology seen on our magnitude images was in general not visible on the phase reconstructions (figure 3), results compatible with those noted on many WM lesions by others.[10,19] Only 1 subpial lesion showed the characteristic phase susceptibility ring observed in some leukocortical lesions.

CNR measurements. FLASH-T2* scans showed the greatest mean ± SE CNR for type I (7.7 ± 1.5), type II (8.6 ± 1.9), and type III/IV (10.5 ± 4) cortical plaques (figure 4). The CNR was lower, though the difference was not significant, for both T2 (type I, 4.3 ± 0.9; type II, 5.1 ± 1.9; type III/IV, 2.5 ± 0.7) and T1 (type I, 4.5 ± 1.8; type II, 3 ± 2.2; type III/IV, 2.9 ± 4.4) scans. Phase images provided the worst contrast for detecting all types of cortical lesions (type I, 0.02 ± 0.4; type II, 1.9 ± 0.9; type III/IV, 0.9 ± 0.4).

When individual types of cortical lesions were considered, the CNR of FLASH-T2* scans was higher ($p < 0.004$, ANOVA) only for type I lesions when compared with the CNR of phase images. However, when all types of lesions were taken into account, the CNR of FLASH-T2* scans was higher than the CNR of T2 ($p < 0.02$), T1 ($p < 0.01$), and phase images ($p < 0.0001$, ANOVA).

Correlation with WM lesion load, demographic characteristics, and clinical characteristics. In patients

Figure 3   Appearance of cortical lesions on phase and magnitude images
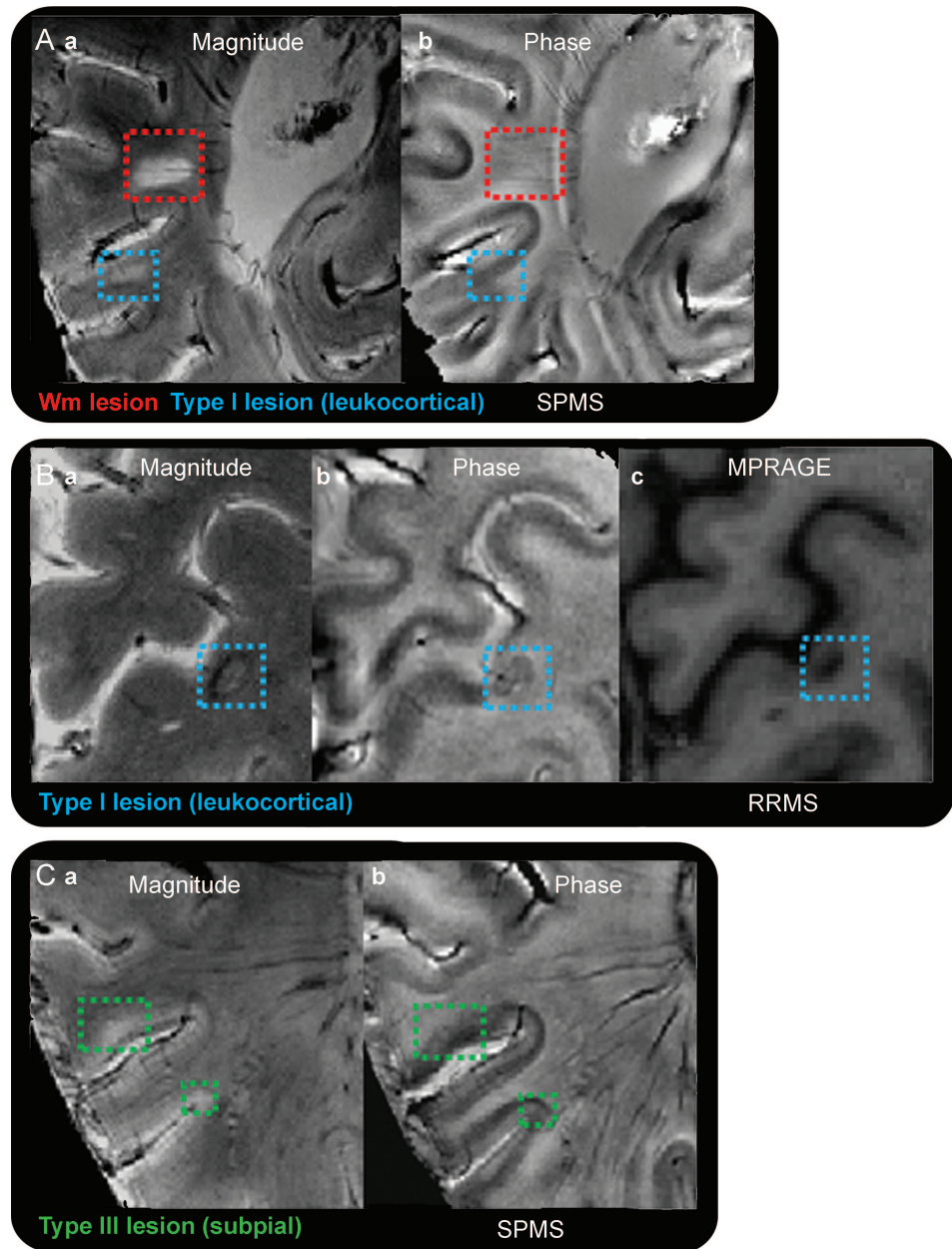

Visualization of (A) white matter (WM; red square) and leukocortical (blue square) lesions on magnitude (a) and phase (b) images in a patient with secondary progressive multiple sclerosis (SPMS); (B) leukocortical lesion (blue square) on magnitude (a), phase (b), and MPRAGE (c) scans of a patient with relapsing–remitting multiple sclerosis (RRMS); and (C) subpial lesions (green squares) on magnitude (a) and phase (b) images of another patient with SPMS. The high-susceptibility χ ring, clearly visible in the leukocortical lesion of the patient with RRMS, was not seen in any of the other lesions in the 2 patients with SPMS. This ring, hypothesized to be due to the expression of iron rich macrophages, may reflect the varying extent of inflammation that characterizes different lesions. MPRAGE = magnetization-prepared rapid gradient echo.

with MS, we did not find any relationship between WM lesion load and the overall number of cortical plaques, as well as with the different lesions types. The total number of cortical lesions as well as the number of type I and type II lesions did not relate to age, disease duration, and disability. However, we found that the higher the number of type III/IV lesions was, the worse the EDSS score was ($p < 0.02$, ρ corre-

lation coefficient: 0.6) and the older the age of patients was ($p < 0.04$, ρ correlation coefficient: 0.5).

DISCUSSION In MS, detection of cortical lesions using currently available MR methods is hindered by the characteristics of these lesions[5,20]—i.e., the lesions are generally small, with sparse inflammatory cell infiltration and blood–brain barrier damage, in
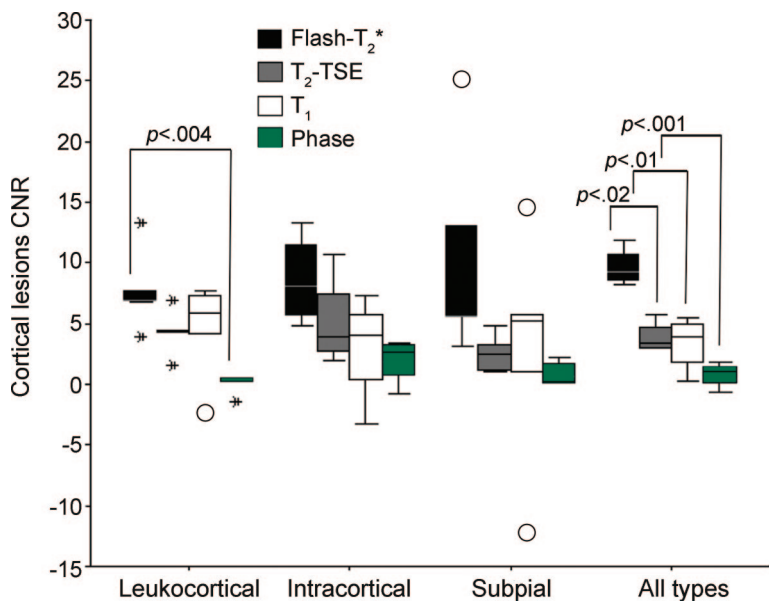
Mean contrast-to-noise ratio (CNR) of different magnetic resonance contrasts of 5 type I, 5 type II, 5 type III/IV, and 15 all types of cortical multiple sclerosis lesions. First, second (median), and third quartiles are used for the box construction, whereas 1.5 × (quartile 3 − quartile 1) is used for the whiskers. The box length is the interquartile range. Points outside the whiskers are considered outliers (cases with values between 1.5 and 3 box lengths from the upper or lower edge of the box). Asterisks represent extreme points (cases with values more than 3 box lengths from the upper or lower edge of the box). FLASH = fast low-angle shot; TSE = turbo spin-echo.

addition to low myelin density in upper cortical layers—as well as by several technical factors, including limited image resolution resulting in partial volume effects with subarachnoid spaces and CSF, and lower contrast between small cortical lesions and surrounding normal cortical GM due to the intrinsically longer GM relaxation times.

The combination of 7-T imaging with multichannel RF technology enabled us to trade off the resultant high SNR for very small voxel volumes, approximately 0.1 mm^3. The high-resolution images acquired allowed us to characterize specific lesion locations inside the cortical ribbon, in analogy to histopathologic lesion typing, and to significantly reduce partial volume effects, especially with adjacent CSF. This may also provide the additional benefit of lessening the need for pulse sequence–based methods (such as fluid-attenuated inversion recovery [FLAIR] and double-inversion recovery [DIR]) designed to mitigate this problem. Of course it is possible that the combination of the higher SNR with such fluid attenuation methods may increase conspicuity even more, once issues of B$_1$ homogeneity and specific absorption rate are addressed at 7 T.

Adequate overall SNR to improve resolution across the cortical sheet provides the capability to

subtype cortical pathology. With these advantages over conventional MRI, we detected lesions with a distribution showing a strong correspondence to that reported by histology.[5,21] This finding, together with the remarkable interrater reproducibility, and, although limited to 1 patient, the high consistency of 7 T in detecting cortical lesions, make us confident that our results are not affected by artifacts. Although our data, of course, cannot be interpreted to mean that ultra-high field MRI can disclose all cortical lesions, they do suggest that the use of 7-T and phased array images provides the ability to detect and characterize all major histologic lesion types with roughly equal capability, including the important class of subpial lesions underestimated by previous studies at lower field strength MRI. Demonstrating the discrepancy between histologic and conventional (1.5-T) MRI data, previous authors found that leukocortical lesions represent the most frequent type of cortical plaques observed on MR scans of patients with MS.[22-24] Relatively recent improvement in MR technology at either 1.5 or 3 T, using FLAIR, DIR, and phase-sensitive inversion recovery imaging either alone or combined with 3-dimensional MPRAGE, increased the potential to directly visualize cortical MS lesions.[25-29] The application of DIR imaging to a large MS population showed a relative improvement in cortical lesion detection compared with more standard clinical sequences (T2-TSE), although a clear differentiation between leukocortical, intracortical, and subpial plaques was not demonstrated.[25]

We characterized the contrast properties of the different types of cortical lesions including T2*-, T2-, T1-weighted, and phase images at 7 T to assess which MR contrasts are more sensitive to cortical pathology. T2*-weighted magnitude images showed the highest, whereas phase images generally the lowest, CNR for all types of cortical lesions. Previous data at ultra-high field MRI, however, have shown that imaging of tissue phase is potentially valuable for defining anatomic structures and improving visualization of the microvasculature.[30,31] Intrinsic tissue iron deposition and microvascular iron seem to contribute to the contrast observed within normal tissues. This increased sensitivity was demonstrated in a small sample of patients with MS who showed a subset of WM plaques with phase contrast only at the peripheral margin of the plaque, a region identified as the zone of inflammation with an influx of iron-rich macrophages.[10,19] The high-susceptibility χ ring was not visible on their corresponding magnitude images. Of all the cortical lesions we observed on magnitude data, only 21% of the leukocortical lesions appeared on phase images and showed phase hypointensity (susceptibility ring) around the pe-

riphery of magnitude hyperintensities. In most of these leukocortical lesions, however, the hypointense ring was already evident on magnitude images. Because we saw similar findings in our WM lesions, the differences between our own and previously reported findings[10,19] are likely attributed to differences in MRI protocols, including the use of longer TE times and thinner slices in our scans, both of which would be expected to increase sensitivity to localized regions of increased microscopic susceptibility effects. Nevertheless, both data sets support the role of phase imaging as a highly sensitive method to characterize the fraction of MS lesions showing evidence of localized high χ zones. The high-susceptibility ring, thought to reflect iron-rich macrophages,[11] may indicate the extent of inflammation in the tissue, which has been reported to be greater in leukocortical vs subpial and intracortical lesions.[5,16,21] Whether this turns out to be a useful biomarker for certain types of plaques or adds insight into the nature of cortical pathology remains to be clarified.

Finally, we explored the relationship between the different types of cortical lesions, WM lesion load, and clinical data. There was no correlation between the volume of focal WM hyperintensities and the number of either overall cortical lesions or each lesion type. However, even in our small patient sample, we found that the higher the number of subpial cortical lesions in patients was, the worse neurologic disability was and the older the age was, reflecting the prevalence of subpial pathology in the progressive forms of MS. Pathologic data showed that patients with a higher number of subpial lesions became wheelchair dependent at a younger age than patients with fewer subpial lesions,[32] suggesting that the frequency and extent of intracortical and subpial demyelination may contribute to disease progression in MS.

Although our findings need to be validated in a larger patients population, they suggest that the use of 7-T MRI in the in vivo study of cortical MS lesions may provide a tool to address important biologic questions unresolved by previous imaging evaluations including the nature of cortical pathology in MS (primary or secondary to WM degeneration), and its impact on the transition to a progressive clinical course. Ultra-high field MRI may also prove to be a valuable tool to assess GM damage in CNS areas other than the cortex and including the spinal cord and the cerebellum as histopathologic examinations described GM demyelination and neuronal pathology in these structures in MS.[33-35]

REFERENCES

1. Taylor E. Zur patologischen anatomie der multiplen sklerose. Dtsch Z Nervenheilkd 1892:1–26.
2. Sander M. Hirnrindenbefunde bei multipler Sklerose. Monatsschr Psych Neurol Neurochir Pol 1898;IV.
3. Brownell B, Hughes J. The distribution of plaques in the cerebrum in multiple sclerosis. J Neurol Neurosurg Psychiatry 1962;25:315–320.
4. Kidd D, Barkhof F, McConnell R, Algra PR, Allen IV, Revesz T. Cortical lesions in multiple sclerosis. Brain 1999;122(pt 1):17–26.
5. Peterson JW, Bo L, Mork S, Chang A, Trapp BD. Transected neurites, apoptotic neurons, and reduced inflammation in cortical multiple sclerosis lesions. Ann Neurol 2001;50:389–400.
6. Stadelmann C, Albert M, Wegner C, Bruck W. Cortical pathology in multiple sclerosis. Curr Opin Neurol 2008; 21:229–234.
7. Vaughan JT, Garwood M, Collins CM, et al. 7T vs. 4T: RF power, homogeneity, and signal-to-noise comparison in head images. Magn Reson Med 2001;46:24–30.
8. Wiggins GC, Potthast A, Triantafyllou C, Wiggins CJ, Wald LL. Eight-channel phased array coil and detunable TEM volume coil for 7 T brain imaging. Magn Reson Med 2005;54:235–240.
9. Novak V, Abduljalil AM, Novak P, Robitaille PM. High-resolution ultrahigh-field MRI of stroke. Magn Reson Imaging 2005;23:539–548.
10. Hammond KE, Lupo JM, Xu D, et al. Development of a robust method for generating 7.0 T multichannel phase images of the brain with application to normal volunteers and patients with neurological diseases. Neuroimage 2008; 39:1682–1692.
11. LeVine SM. Iron deposits in multiple sclerosis and Alzheimer's disease brains. Brain Res 1997;760:298–303.
12. McDonald WI, Compston A, Edan G, et al. Recommended diagnostic criteria for multiple sclerosis: guide-

lines from the International Panel on the Diagnosis of Multiple Sclerosis. Ann Neurol 2001;50:121–127.

13. Kurtzke JF. Rating neurologic impairment in multiple sclerosis: an Expanded Disability Status Scale (EDSS). Neurology 1983;33:1444–1452.

14. Sled JG, Zijdenbos AP, Evans AC. A nonparametric method for automatic correction of intensity nonuniformity in MRI data. IEEE Trans Med Imaging 1998; 17:87–97.

15. Jenkinson M. Fast, automated, N-dimensional phase-unwrapping algorithm Magn Reson Med 2003;49:193–197.

16. Bo L, Vedeler CA, Nyland H, Trapp BD, Mork SJ. Intracortical multiple sclerosis lesions are not associated with increased lymphocyte infiltration. Mult Scler 2003;9:323–331.

17. Vercellino M, Plano F, Votta B, Mutani R, Giordana MT, Cavalla P. Grey matter pathology in multiple sclerosis. J Neuropathol Exp Neurol 2005;64:1101–1107.

18. Mainero C, De Stefano N, Iannucci G, et al. Correlates of MS disability assessed in vivo using aggregates of MR quantities. Neurology 2001;56:1331–1334.

19. Hammond KE, Metcalf M, Carvajal L, et al. Quantitative in vivo magnetic resonance imaging of multiple sclerosis at 7 Tesla with sensitivity to iron. Ann Neurol 2008;64:707–713.

20. Bo L, Geurts JJ, Mork SJ, van der Valk P. Grey matter pathology in multiple sclerosis. Acta Neurol Scand Suppl 2006;183:48–50.

21. Wegner C, Esiri MM, Chance SA, Palace J, Matthews PM. Neocortical neuronal, synaptic, and glial loss in multiple sclerosis. Neurology 2006;67:960–967.

22. Geurts JJ, Bo L, Pouwels PJ, Castelijns JA, Polman CH, Barkhof F. Cortical lesions in multiple sclerosis: combined postmortem MR imaging and histopathology. AJNR Am J Neuroradiol 2005;26:572–577.

23. Bagnato F, Butman JA, Gupta S, et al. In vivo detection of cortical plaques by MR imaging in patients with multiple sclerosis. AJNR Am J Neuroradiol 2006;27:2161–2167.

24. Bakshi R, Ariyaratana S, Benedict RH, Jacobs L. Fluid-attenuated inversion recovery magnetic resonance imaging detects cortical and juxtacortical multiple sclerosis lesions. Arch Neurol 2001;58:742–748.

25. Calabrese M, De Stefano N, Atzori M, et al. Detection of cortical inflammatory lesions by double inversion recovery magnetic resonance imaging in patients with multiple sclerosis. Arch Neurol 2007;64:1416–1422.

26. Calabrese M, De Stefano N, Atzori M, et al. Extensive cortical inflammation is associated with epilepsy in multiple sclerosis. J Neurol 2008;255:581–586.

27. Nelson F, Poonawalla A, Hou P, Wolinsky JS, Narayana PA. 3D MPRAGE improves classification of cortical lesions in multiple sclerosis. Mult Scler 2008;14:1214–1219.

28. Nelson F, Poonawalla AH, Hou P, Huang F, Wolinsky JS, Narayana PA. Improved identification of intracortical lesions in multiple sclerosis with phase-sensitive inversion recovery in combination with fast double inversion recovery MR imaging. AJNR Am J Neuroradiol 2007;28:1645–1649.

29. Wattjes MP, Lutterbey GG, Gieseke J, et al. Double inversion recovery brain imaging at 3T: diagnostic value in the detection of multiple sclerosis lesions. AJNR Am J Neuroradiol 2007;28:54–59.

30. Duyn JH, van Gelderen P, Li TQ, de Zwart JA, Koretsky AP, Fukunaga M. High-field MRI of brain cortical substructure based on signal phase. Proc Natl Acad Sci USA 2007;104:11796–11801.

31. Haacke EM, Mittal S, Wu Z, Neelavalli J, Cheng YC. Susceptibility-weighted imaging: technical aspects and clinical applications, part 1. AJNR Am J Neuroradiol 2009;30:19–30.

32. Magliozzi R, Howell O, Vora A, et al. Meningeal B-cell follicles in secondary progressive multiple sclerosis associate with early onset of disease and severe cortical pathology. Brain 2007;130:1089–1104.

33. Kutzelnigg A, Faber-Rod JC, Bauer J, et al. Widespread demyelination in the cerebellar cortex in multiple sclerosis. Brain Pathol 2007;17:38–44.

34. Gilmore CP, Bo L, Owens T, Lowe J, Esiri MM, Evangelou N. Spinal cord gray matter demyelination in multiple sclerosis: a novel pattern of residual plaque morphology. Brain Pathol 2006;16:202–208.

35. Gilmore CP, Deluca GC, Bo L, et al. Spinal cord neuronal pathology in multiple sclerosis. Brain Pathol Epub 2008 Dec 19.

Resident & Fellow Section: Call for Teaching Videos

The *Neurology*® Resident section is featured online at www.neurology.org. The Editorial Team of this section is seeking teaching videos that will illustrate classic or uncommon findings on movement disorders. Such videos will aid in the recognition of such disorders. Instructions for formatting videos can be found in the Information for Authors at www.neurology.org.